

SepViT: Separable Vision Transformer

Wei Li^{1,2,†*}, Xing Wang^{2,*}, Xin Xia², Jie Wu²,
Jiashi Li², Xuefeng Xiao², Min Zheng², Shiping Wen³

¹ University of Electronic Science and Technology of China

² ByteDance Inc, ³ University of Technology Sydney

Abstract

Vision Transformers have witnessed prevailing success in a series of vision tasks. However, these Transformers often rely on extensive computational costs to achieve high performance, which is burdensome to deploy on resource-constrained devices. To alleviate this issue, we draw lessons from depthwise separable convolution and imitate its ideology to design an efficient Transformer backbone, i.e., *Separable Vision Transformer*, abbreviated as *SepViT*. *SepViT* helps to carry out the local-global information interaction within and among the windows in sequential order via a depthwise separable self-attention. The novel window token embedding and grouped self-attention are employed to compute the attention relationship among windows with negligible cost and establish long-range visual interactions across multiple windows, respectively. Extensive experiments on general-purpose vision benchmarks demonstrate that *SepViT* can achieve a state-of-the-art trade-off between performance and latency. Among them, *SepViT* achieves 84.2% top-1 accuracy on ImageNet-1K classification while decreasing the latency by 40%, compared to the ones with similar accuracy (e.g., CSWin). Furthermore, *SepViT* achieves 51.0% mIoU on ADE20K semantic segmentation task, 47.9 AP on the RetinaNet-based COCO detection task, 49.4 box AP and 44.6 mask AP on Mask R-CNN-based COCO object detection and instance segmentation tasks. The code is available at: <https://github.com/liwei109/SepViT>.

Introduction

Recently, many computer vision researchers make efforts to design CV-oriented vision Transformer to surpass the performance of the convolutional neural networks (CNNs). Due to a high capability in modeling the long-range dependencies, vision Transformer achieves prominent results in diversified vision tasks, such as image classification (Dosovitskiy et al. 2020; Touvron et al. 2021; Han et al. 2021; Liu et al. 2021; Chu et al. 2021a; Dong et al. 2021), semantic segmentation (Xie et al. 2021; Zheng et al. 2021; Wang et al. 2021a), object detection (Carion et al. 2020; Zhu et al. 2020; Dai et al. 2021) and etc. However, the powerful performance usually comes at a cost of heavy computational complexity.

Primordially, ViT (Dosovitskiy et al. 2020) firstly introduces Transformer to the image recognition tasks. It splits

the whole image into patches and feeds each patch as a token into Transformer. However, the patch-based Transformer is hard to deploy due to the computationally inefficient full-attention mechanism. To relieve this problem, Swin (Liu et al. 2021) proposes the window-based self-attention to limit the computation of self-attention in non-overlapping sub-windows. Obviously, the window-based self-attention helps to reduce the complexity to a great extent, but the shifted operator for building connection among the windows brings difficulty for ONNX or TensorRT deployment. Twins (Chu et al. 2021a) takes advantage of the window-based self-attention and the spatial reduction attention from PVT (Wang et al. 2021c) and proposes the spatially separable self-attention. Although Twins is deployment-friendly and achieves outstanding performance, its computational complexity is hardly reduced. CSWin (Dong et al. 2021) shows state-of-the-art performance via the novel cross-shaped window self-attention, but its throughput is low. Albeit, with varying degrees of progress in these famous vision Transformers, most of its recent successes are accompanied with huge resource demands.

To overcome the aforementioned issues, we propose an efficient Transformer backbone, called Separable Vision Transformer (SepViT), which captures both local and global dependencies in a sequential order. A key design element of SepViT is its depthwise separable self-attention module, as shown in Fig. 2. Inspired by the depthwise separable convolution in MobileNets (Howard et al. 2017; Sandler et al. 2018; Howard et al. 2019), we re-design the self-attention module and propose the depthwise separable self-attention, which consists of a depthwise self-attention (PSA) and a pointwise self-attention (PSA) that can correspond to depthwise and pointwise convolution in MobileNets, respectively. The depthwise self-attention is used to capture local feature within each window while the pointwise self-attention is for building connections among windows that notably improve the expressive power. Moreover, to get the global representation of a local window, we develop a novel window token embedding, which is utilized to compute the attention relationship among windows. Furthermore, we also extend the idea of grouped convolution from AlexNet (Krizhevsky, Sutskever, and Hinton 2012) to our depthwise separable self-attention and present the grouped self-attention to further improve the performance.

*Corresponding Authors. †Intern at ByteDance.

Email: liwei9719@126.com, wangxing.613@bytedance.com

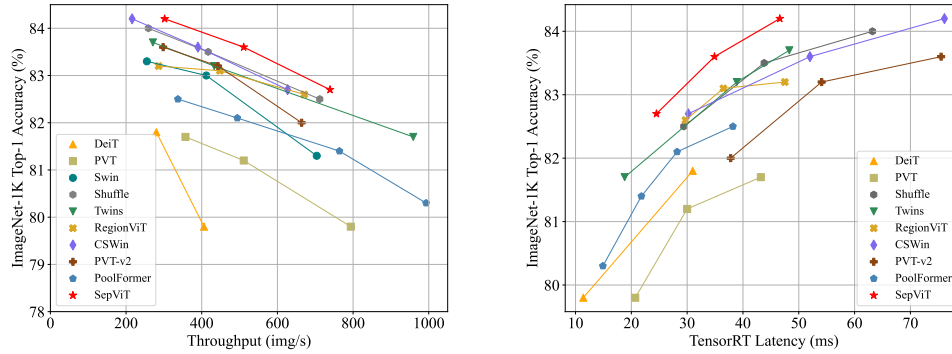


Figure 1: Comparison of throughput and latency on ImageNet-1K classification. The throughput and the latency are tested based on the PyTorch and TensorRT framework, respectively.

To demonstrate the effectiveness of SepViT, we conduct a series of experiments on some typical vision tasks, including ImageNet-1K (Russakovsky et al. 2015) classification, ADE20K (Zhou et al. 2017) semantic segmentation, COCO (Lin et al. 2014) object detection and instance segmentation. The experimental results show that SepViT can achieve a better trade-off between performance and latency than other competitive vision Transformers (Wang et al. 2021c; Liu et al. 2021; Chu et al. 2021a; Dong et al. 2021). As shown in Fig. 1, SepViT achieves better accuracy at the same throughput or latency constraint, and costs less inference time than the methods with the same accuracy. Furthermore, SepViT can be expediently applied and deployed since it only contains some universal operators (e.g., transpose and matrix multiplication). Formally, the contributions of our work can be summarized as follows:

1. We design a lightweight yet efficient depthwise separable self-attention and extend it to grouped self-attention, which can achieve the information interaction within and among windows in a single Transformer block.
2. We present the window token embedding to learn a global feature representation of each window, which is used to build the attention relationship among windows with negligible computational cost.
3. We propose an efficient Separable Vision Transformer (SepViT), which achieves a state-of-the-art trade-off between performance and latency on various vision tasks.

Related work

Vision Transformer

Vision Transformer first comes into our view when ViT (Dosovitskiy et al. 2020) is born and achieves an excellent performance on classification task. In quick succession, a series of vision Transformers have been produced based on ViT, such as DeiT (Touvron et al. 2021), T2T (Yuan et al. 2021), TNT (Han et al. 2021), CPVT (Chu et al. 2021b), etc. Later, PVT (Wang et al. 2021c) and Swin (Liu et al. 2021) synchronously propose the hierarchical architecture which is friendly for the dense prediction tasks,

such as object detection, semantic and instance segmentation. Meanwhile, Swin (Liu et al. 2021) as a pioneer proposes the window-based self-attention to compute attention within local windows. Soon after, Twins (Chu et al. 2021a) and CSWin (Dong et al. 2021) sequentially propose the spatial separable self-attention and cross-shaped window self-attention based on the hierarchical architecture. On the other hand, some researchers incorporate the spatial inductive biases of CNNs into Transformer. CoaT (Xu et al. 2021), CVT (Wu et al. 2021) and LeViT (Graham et al. 2021) introduce the convolutions before or after self-attentions and obtain well-pleasing results. Regarding to the design of lightweight Transformer, MobileFormer (Chen et al. 2021d) and MobileViT (Mehta and Rastegari 2021) combine Transformer blocks with the inverted bottleneck blocks in MobileNet-V2 (Sandler et al. 2018) in series and parallel. Besides, another direction of research (So, Le, and Liang 2019; Chen et al. 2021c,a; Li et al. 2021) is to automatically search the structure details of Transformer with neural architecture search (Zoph and Le 2016; Li et al. 2022) technology.

Lightweight Convolutions

Many lightweight and mobile-friendly convolutions are proposed for mobile vision tasks. Of these, grouped convolution is the first to be proposed by AlexNet (Krizhevsky, Sutskever, and Hinton 2012), which groups the feature maps and conducts the distributed training. Then the representative work of mobile-friendly convolution must be the MobileNets (Howard et al. 2017; Sandler et al. 2018; Howard et al. 2019) with depthwise separable convolution, which contains a depthwise convolution for spatial information communication and a pointwise convolution for information exchange across the channels. As time goes on, plenty of variants based on the aforementioned works are developed, such as (Zhang et al. 2018; Ma et al. 2018; Tan and Le 2019; Han et al. 2020). In our work, we adapt the ideology of depthwise separable convolution to Transformer, which aims to reduce the Transformer’s computational complexity without the sacrifice of performance.

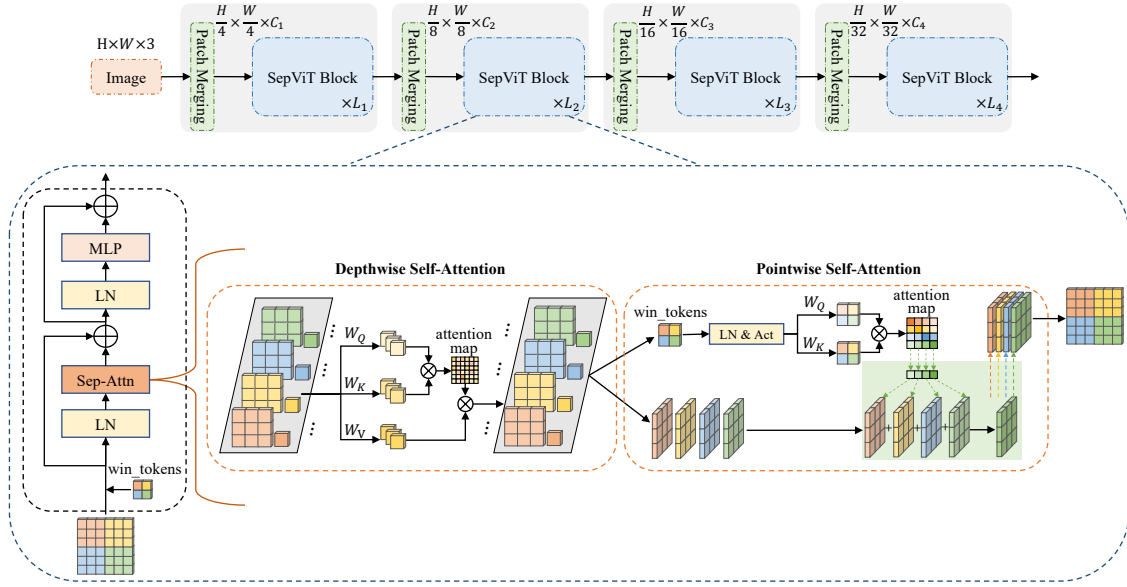


Figure 2: Separable Vision Transformer (SepViT). Top row is the overall hierarchical architecture of SepViT. Bottom row is the SepViT block and detailed visualization of our depthwise separable self-attention and the window token embedding scheme.

SepViT

In this section, we first illustrate the design overview for SepViT, and then discuss some key modules within the SepViT block. Finally, we provide the architecture specifications and variants with different model sizes.

Overview

As illustrated in Fig. 2, SepViT follows the widely-used hierarchical architecture (Wang et al. 2021c; Liu et al. 2021; Chu et al. 2021a; Dong et al. 2021) and the window-based self-attention (Liu et al. 2021). Besides, SepViT also employs conditional position encoding (CPE) from (Chu et al. 2021b,a). For each stage, there is an overlapping patch merging layer for feature map downsampling followed by a series of SepViT blocks. The spatial resolution will be progressively reduced by $32\times$ with either stride 4 or 2, and the channel dimension will be doubled stage by stage. It is worth noting that both local contextual concepts and global abstraction can be captured in a single SepViT block, while other works (Liu et al. 2021; Chu et al. 2021a) should employ two successive blocks to accomplish this local-global modeling. In the SepViT block, local information communication within each window is achieved by depthwise self-attention (DSA), and global information exchange among the windows is performed via pointwise self-attention (PSA).

Depthwise Separable Self-Attention

Depthwise Self-Attention (DSA). Similar to some pioneering works (Liu et al. 2021; Chu et al. 2021a), SepViT is built on top of the window-based self-attention scheme. Firstly, we perform a window partition on the input feature map. Each window can be seen as an input channel of the

feature map, while different windows contain diverse information. Different from previous works, we create a window token for each window, which serves as a global representation and is used to model the attention relationship in the following pointwise self-attention module.

Then, a depthwise self-attention (DSA) is performed on all the pixel tokens within each window as well as its corresponding window token. This window-wise operation is quite similar to a depthwise convolution layer in MobileNets, aiming to fuse the spatial information within each channel. Besides, a residual short cut is employed for DSA to prevent information loss. The implementation of DSA can be summarized as follows:

$$\text{DSA}(z) = \text{Attention}(z \cdot W_Q, z \cdot W_K, z \cdot W_V) + z \quad (1)$$

where z is the feature tokens, consisted of the pixel tokens and window tokens. W_Q , W_K , and W_V denote three Linear layers for query, key and value computation in a regular self-attention. Attention means a standard self-attention operator performing as: $\text{Attention}(Q, K, V) = \text{softmax}(\frac{QK^T}{d_k})V$, in which d_k denotes scaling factor. Here, it works on the each of the local window.

Window Token Embedding. To establish the attention relationship among windows, a straightforward solution is to employ all pixel tokens of each window. However, it will bring huge computational costs and lead the whole model to be complex. To alleviate this issue, we present a window token embedding scheme, which leverages a single token to encapsulate the core information for each sub-window. This window token can be initialized either as a fixed zero vector or a learnable vector. While passing through DSA, there is an informational interaction between the window token and pixel tokens in each window. Thus the window token can

learn a global representation of this window. Thanks to the effective window token, we can build the attention relationship among windows with negligible computational cost.

Pointwise Self-Attention (PSA). The famous pointwise convolution in MobileNets is utilized to fuse the information from different channels. In our work, we imitate pointwise convolution to develop the pointwise self-attention (PSA) module to establish connections among windows. PSA is mainly used to fuse the information across windows and obtain a final representation of the input feature map as well. More specifically, we extract the feature maps and window tokens from the output of DSA. Then, window tokens are used to compute the attention relationship among windows and generate the attention map after a LayerNormalization (LN) layer and a GELU activation function (Act). Meanwhile, we directly treat the feature maps as the value branch of PSA without any other extra operation.

With the attention map and the feature maps which are in the form of windows, we perform an attention computation among the windows for global information exchange. PSA adopts a residual connection as well. Formally, the implementation of PSA can be depicted as follows:

$$\text{PSA}(z, wt) = \text{Attention}(\text{GELU}(\text{LN}(wt)) \cdot W_Q, \text{GELU}(\text{LN}(wt)) \cdot W_K, z) + z \quad (2)$$

where wt denotes the window token. Here, Attention is a standard self-attention operator as well, but works on the whole feature maps that are in the form of windows z .

Complexity Analysis. Given an input feature with size $H \times W \times C$, the computational complexity of the multi-head self-attention (MSA) is $4HWC^2 + 2H^2W^2C$ in the global Transformer block of ViT (Dosovitskiy et al. 2020). The complexity of the MSA in a window-based Transformer with window size $M \times M$ (Usually, M is a common factor of H and W , so the number of the windows is $N = \frac{HW}{M^2}$) can be decreased to $4HWC^2 + 2M^2HWC$ in Swin (Liu et al. 2021). As for the depthwise separable self-attention in SepViT, the complexity contains two parts, DSA and PSA.

DSA. Building on top of a window-based self-attention, DSA shares a similar computational cost to it. Additionally, the introduction of window tokens will cause an extra cost, but it is negligible compared to the overall cost of DSA. The complexity of DSA can be calculated as follows:

$$\Omega(\text{DSA}) = 3HWC^2 + 3NC^2 + 2N(M^2 + 1)^2C \quad (3)$$

where $3NC^2$ is the extra cost of encoding window tokens in Linear layers. $2N(M^2 + 1)^2C$ indicates the matrix multiplications involved in the self-attention for N windows, where $M^2 + 1$ represents the M^2 pixel tokens in a window and its corresponding window token. Thanks to that the number of sub-windows N is usually a small value, the extra costs caused by window tokens can be ignored.

PSA. Since the window token summarizes the global information of a local window, the proposed PSA helps to efficiently perform information exchange among windows in a window level instead of pixel level. Concretely, the complexity of PSA is given as follows:

$$\Omega(\text{PSA}) = HWC^2 + 2NC^2 + N^2C + NHWC \quad (4)$$

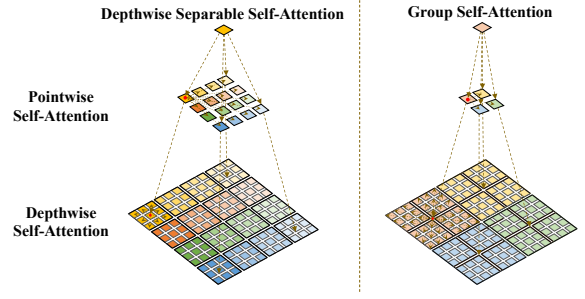


Figure 3: A macro view of the similarities and differences between the depthwise separable self-attention and the grouped self-attention.

where $2NC^2$ represents the little cost of computing the query and key with N window tokens, while the value branch is zero-cost. N^2C indicates the computation of generating attention map with N window tokens in a window level, which saves computational cost for PSA to a great extent. Finally, $NHWC$ indicates the matrix multiplication between the attention map and the feature maps.

Grouped Self-Attention

Motivated by the excellent performance of grouped convolution in visual recognition (Krizhevsky, Sutskever, and Hinton 2012), we make an extension of our depthwise separable self-attention and propose the grouped self-attention. As shown in Fig. 3, we splice several neighboring sub-windows to form a larger window, which is similar to dividing the windows into groups and conducting a depthwise self-attention communication inside a group of windows. In this way, the grouped self-attention can capture long-range visual dependencies of multiple windows. In terms of computational cost and performance gains, the grouped self-attention has a certain extra cost compared with the depthwise separable self-attention but results in a better performance. Ultimately, we apply the block with grouped self-attention (GSA) to SepViT and run it alternately with the depthwise separable self-attention block (DSSA) in the late stages of the network.

SepViT Block

Formally, our SepViT block can be formulated as follows:

$$\tilde{z}^l = \text{Concat}(z^{l-1}, wt) \quad (5)$$

$$\hat{z}^l = \text{DSA}(\text{LN}(\tilde{z}^l)) \quad (6)$$

$$\dot{z}^l, \dot{wt} = \text{Slice}(\hat{z}^l) \quad (7)$$

$$\hat{z}^l = \text{PSA}(\dot{z}^l, \dot{wt}) + z^{l-1} \quad (8)$$

$$z^l = \text{MLP}(\text{LN}(\hat{z}^l)) + \hat{z}^l \quad (9)$$

where \tilde{z}^l , \hat{z}^l and z^l denote the outputs of the DSA, PSA and SepViT block l , respectively. \tilde{z}^l and wt are feature maps and the learned window tokens. Concat represents the concatenation operation while Slice represents the slice operation.

Comparison of Complexity and Inference Speed. We compare SepViT block (DSSA) with two other SOTA blocks

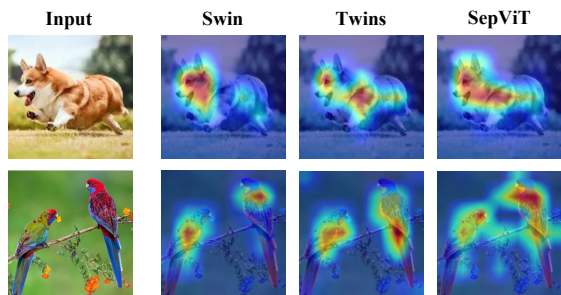


Figure 4: Grad-CAM (Selvaraju et al. 2017) activation maps of Swin-T, Twins-SVT-S and SepViT-T. SepViT shows a prominent capability of capturing a wider range information.

(Swin (Liu et al. 2021), Twins (Chu et al. 2021a)). As we stated before, the information interaction within and among windows is completed in a single SepViT block, while Swin (Liu et al. 2021) and Twins (Chu et al. 2021a) require two successive blocks. As shown in Table 1, we can observe that the SepViT block only costs about half the MACs of its competitors. The reason lies in two aspects. Firstly, SepViT block is more lightweight. Secondly, SepViT block removes many redundant layers, e.g., there is only one MLP layer and two LN layers in a single SepViT block while there are double MLP and LN layers in two successive Swin or Twins blocks. On the other hand, we make a comparison of inference speed between a single SepViT block with these two-block pattern works (Swin and Twins). Table 1 reports that SepViT block is about 60% faster on Pytorch and 55% faster on TensorRT.

Block Type	FLOPs(G)	Throughput(img/s)	Latency(ms)
Swin	0.77	1346	-
Twins	0.78	1403	5.3
SepViT	0.40	2146	2.4

Table 1: Comparison of complexity and inference speed between SepViT block and the two-block pattern works.

Experimental Results

To present a fair comparison with other ViTs, we mainly propose the SepViT-T/S/B variants. A series of experiments are conducted with them to verify the capability of SepViT, including classification, segmentation and detection. Architecture configurations and implementation details are provided in Appendix.

ImageNet-1K Classification

We first carry out the image classification experiment on the ImageNet-1K (Russakovsky et al. 2015). As the results shown in Table 2, compared to the latest state-of-the-art vision Transformers, SepViT achieves the best trade-off between accuracy and latency. To be more specific, compared with these famous ViTs (e.g. Swin), SepViT-S/B achieve 83.6% and 84.2% top-1 accuracy surpassing Swin-S/B by

Method	Param (M)	FLOPs (G)	Throughput (img/s)	Latency (ms)	Top-1 Acc (%)
ConvNet					
ConvNeXt-T(Liu et al. 2022)	29.0	4.5	-	19.0	82.1
ConvNeXt-S(Liu et al. 2022)	50.0	8.7	-	28.1	83.1
ConvNeXt-B(Liu et al. 2022)	88.0	15.4	-	37.3	83.9
Transformer					
DeiT-Small/16(Touvron et al. 2021)	22.0	4.6	406	11.4	79.9
T2T-ViT-14(Yuan et al. 2021)	22.0	5.2	-	-	81.5
TNT-S(Han et al. 2021)	23.8	5.2	-	-	81.3
CoaT-Lite-Small(Xu et al. 2021)	20.0	4.0	-	-	81.9
CvT-13(Wu et al. 2021)	20.0	4.5	-	-	81.6
PVT-Small(Wang et al. 2021c)	24.5	3.8	794	20.7	79.8
Swin-T(Liu et al. 2021)	29.0	4.5	704	-	81.3
Shuffle-T(Huang et al. 2021)	29.0	4.6	712	29.4	82.5
Twins-S(Chu et al. 2021a)	24.0	2.9	979	18.8	81.7
RegionViT-S(Chen et al. 2021b)	40.6	5.3	671	29.7	82.6
CSWin-T(Dong et al. 2021)	23.0	4.3	627	30.2	82.7
PVT-v2-B2(Wang et al. 2021b)	25.4	4.0	664	37.8	82.0
PoolFormer-S24(Yu et al. 2022)	21.0	3.5	993	14.9	80.3
PoolFormer-S36(Yu et al. 2022)	31.0	5.1	764	21.8	81.4
SepViT-T(ours)	31.2	4.5	729	24.5	82.7
T2T-ViT-19(Yuan et al. 2021)	39.2	8.9	-	-	81.9
CoaT-Lite-Medium(Xu et al. 2021)	45.0	9.8	-	-	83.6
CvT-21(Wu et al. 2021)	32.0	7.1	-	-	82.5
CMT-S(Guo et al. 2021)	25.1	4.0	-	52.0	83.5
PVT-Medium(Wang et al. 2021c)	44.2	6.7	511	30.0	81.2
Swin-S(Liu et al. 2021)	50.0	8.7	412	-	83.0
Shuffle-S(Huang et al. 2021)	50.0	8.9	417	43.8	83.5
Twins-B(Chu et al. 2021a)	56.0	8.6	433	38.9	83.2
RegionViT-M(Chen et al. 2021b)	41.2	7.4	448	36.5	83.1
CSWin-S(Dong et al. 2021)	35.0	6.9	390	52.0	83.6
PVT-v2-B3(Wang et al. 2021b)	45.2	6.9	443	54.1	83.2
PoolFormer-M36(Yu et al. 2022)	56.0	9.0	494	28.2	82.1
SepViT-S(ours)	46.6	7.5	471	34.9	83.6
DeiT-Base/16(Touvron et al. 2021)	86.6	17.6	273	31.0	81.8
T2T-ViT-24(Yuan et al. 2021)	64.1	14.1	-	-	82.3
TNT-B(Han et al. 2021)	66.0	14.1	-	-	82.8
PVT-Large(Wang et al. 2021c)	61.4	9.8	357	43.2	81.7
Swin-B(Liu et al. 2021)	88.0	15.4	255	-	83.3
Shuffle-B(Huang et al. 2021)	88.0	15.6	259	63.2	84.0
Twins-L(Chu et al. 2021a)	99.2	15.1	271	48.3	83.7
RegionViT-B(Chen et al. 2021b)	72.7	13.0	286	47.5	83.2
CSWin-B(Dong et al. 2021)	78.0	15.0	216	76.1	84.2
PVT-v2-B4(Wang et al. 2021b)	62.6	10.1	298	75.5	83.6
PoolFormer-M48(Yu et al. 2022)	73.0	11.8	337	38.2	82.5
SepViT-B(ours)	82.3	13.1	302	46.6	84.2

Table 2: Comparison of different state-of-the-art methods on ImageNet-1K classification. Throughput and latency are tested based on the PyTorch framework with a V100 GPU (batch size=192) and TensorRT framework with a T4 GPU (batch size=8).

0.6% and 0.9% with about 14% fewer FLOPs and 15% faster inference speed. As for the tiny variant, SepViT-T outperforms the Swin-T by 1.4% with the same FLOPs of 4.5G and a faster throughput as well. Meanwhile, SepViT-T/S/B outperforms RegionViT-S/M/B by 1.1%, 0.5% and 1.0% under a similar TensorRT latency. On the other hand, compared with the recent SOTA methods with the similar accuracy (e.g. CSWin and Shuffle Transformer), both of our small and base variants cost about 40% less inference latency on TensorRT than CSWin-S/B, and SepViT-T is 19% faster than CSWin-T as well. Compared to Shuffle Transformer, SepViT-T/S/B achieve a better performance than Shuffle-T/S/B while being 17%, 20% and 27% faster on TensorRT. Moreover, SepViT also shows very a promising performance by comparing with the CNNs counterparts under the similar FLOPs (e.g. RegNetY and ConvNeXt).

Semantic Segmentation

To further verify the capacity of SepViT, we conduct the semantic segmentation experiment on ADE20K (Zhou et al. 2017). In Table 3, we make a comparison with the recent

Backbone	Latency (ms)	Semantic FPN 80k			UperNet 160k			
		Param(M)	FLOPs(G)	mIoU(%)	Param(M)	FLOPs(G)	mIoU/MS	mIoU(%)
ResNet50(He et al. 2016)	18.8	28.5	183	36.7	-	-	-/-	
ConvNeXt-T(Liu et al. 2022)	78.5	-	-	-	60.0	939	-/46.7	
PVT-Small(Wang et al. 2021c)	129.6	28.2	161	39.8	-	-	-/-	
Swin-T(Liu et al. 2021)	-	31.9	182	41.5	59.9	945	44.5/45.8	
Shuffle-T(Huang et al. 2021)	168.9	-	-	-	60.0	-	46.6/47.6	
Twins-S(Chu et al. 2021a)	127.2	28.3	144	43.2	54.4	901	46.2/47.1	
PoolFormer-S36(Yu et al. 2022)	87.7	34.6	-	42.0	-	-	-/-	
SepViT-T(ours)	139.7	38.8	181	44.8	66.8	940	47.4/48.3	
ResNet101(He et al. 2016)	32.8	47.5	260	38.8	86.0	1092	-/44.9	
ConvNeXt-S(Liu et al. 2022)	131.5	-	-	-	82.0	1027	-/49.6	
PVT-Medium(Wang et al. 2021c)	184.2	48.0	219	41.6	-	-	-/-	
Swin-S(Liu et al. 2021)	-	53.2	274	45.2	81.3	1038	47.6/49.5	
Shuffle-S(Huang et al. 2021)	283.7	-	-	-	81.0	-	48.4/49.6	
Twins-B(Chu et al. 2021a)	231.8	60.4	261	45.3	88.5	1020	47.7/48.9	
PoolFormer-M36(Yu et al. 2022)	127.8	59.8	-	42.4	-	-	-/-	
SepViT-S(ours)	201.5	55.4	244	46.6	83.4	1003	48.6/49.9	
ResNeXt101-64×4d(Xie et al. 2017)	65.7	86.4	-	40.2	-	-	-/-	
ConvNeXt-B(Liu et al. 2022)	181.3	-	-	-	122.0	1170	-/49.9	
PVT-Large(Wang et al. 2021c)	359.3	65.1	283	42.1	-	-	-/-	
Swin-B(Liu et al. 2021)	-	91.2	422	46.0	121.0	1188	48.1/49.7	
Shuffle-B(Huang et al. 2021)	521.2	-	-	-	121.0	-	49.0/50.5	
Twins-L(Chu et al. 2021a)	409.7	103.7	404	46.7	133.0	1164	48.8/49.7	
PoolFormer-M48(Yu et al. 2022)	168.7	77.1	-	42.7	-	-	-/-	
SepViT-B(ours)	366.3	94.7	367	47.6	124.8	1128	49.6/51.0	

Table 3: Comparison of different backbones on ADE20K semantic segmentation task. Latency is the TensorRT runtime of the backbone with the input size of 512×512 (batch size=8). FLOPs are measured with the input size of 512×2048 .

vision Transformer and CNN backbones. Based on the Semantic FPN framework (Kirillov et al. 2019), SepViT-T/S/B surpasses Swin-T/S/B by 3.3%, 1.4% and 1.6% mIoU with fewer FLOPs, and outperforms Twins-S/B/L by 1.6%, 1.3% and 0.9% mIoU with faster TensorRT inference time. Meanwhile, SepViT shows great advantage over CNNs. SepViT-T/S gain a promising performance of 8.1% and 7.8% mIoU than ResNet50 and ResNet101. By contrast with Swin on the UperNet framework (Xiao et al. 2018), SepViT-T/S/B achieves 2.9%, 1.0%, 1.5% higher mIoU on single-scale testing and 2.5%, 0.4%, 1.3% higher mIoU in terms of multi-scale (MS) testing. Compared to the famous ConvNeXt, SepViT-T/S/B achieve 1.6%, 0.3% and 1.1% higher mIoU on multi-scale testing. Extensive experiments reveal that SepViT shows great potential on segmentation tasks.

Object Detection and Instance Segmentation

Next, we evaluate SepViT on the objection detection and instance segmentation tasks with RetinaNet (Lin et al. 2017) and Mask R-CNN (He et al. 2017) frameworks on COCO (Lin et al. 2014). The experimental results in Table 4 show that SepViT achieves a state-of-the-art performance compared with the recent vision Transformers and some famous CNNs, and its TensorRT runtime is competitive as well. Based on the RetinaNet framework, SepViT-T/S surpass Swin-T/S by 3.3, 1.9 AP with fewer FLOPs in the $1 \times$ experiment. For the $3 \times$ schedule, SepViT-S outperforms Twins-B and RegionViT-B by 1.0 and 1.8 AP with a faster inference speed at the same time. As for the Mask R-CNN framework, SepViT-T outperforms Swin-T by 3.3 AP^b, 2.8 AP^m with $1 \times$ schedule, and 2.0 AP^b, 2.2 AP^m with $3 \times$

schedule. For the SepViT-S variant, it achieves a similar performance gain while saving a certain amount of computation overhead and inference latency. Furthermore, compared with the famous CNNs in the $3 \times$ experiment, SepViT-T surpasses ConvNeXt-T by 1.8 AP^b, 2.1 AP^m, and SepViT-S outperforms ResNet101 by 6.6 AP^b, 6.1 AP^m. Thus, experimental results on these object detection and instance segmentation tasks demonstrate SepViT’s capability of getting better trade-off between performance and latency.

Ablation Study

To better demonstrate the significance of each key component, including depthwise separable self-attention, grouped self-attention and window token embedding scheme in SepViT, we conduct a series of ablation experiments on ImageNet-1K classification with SepViT-T variant.

Efficient Components. As mentioned above, SepViT adopts the conditional position encoding (CPE) (Chu et al. 2021b). Therefore, we take the Swin-T+CPVT reported in (Chu et al. 2021a) as the baseline. As shown in Table 5 where each component is added in turn to verify their benefits, SepViT-T simply equipped with the depthwise separable self-attention block (DSSA) outperforms Swin+CPVT by 1.0% (from 81.2% to 82.2%) and it is much faster with the throughput of 740 images/s. After employing grouped self-attention block (GSA) and DSSA alternately in the second and third stages, we gain an accuracy improvement of 0.3% (from 82.2% to 82.5%). Moreover, we study whether it makes a difference if the window token is initialized with a fixed zero vector or a learnable vector. In contrast to the

Backbone	Latency (ms)	RetinaNet				Mask R-CNN					
		Params (M)	FLOPs (G)	1×	3× + MS	Params (M)	FLOPs (G)	1×		3× + MS	
				AP	AP			AP ^b	AP ^m	AP ^b	AP ^m
ResNet50(He et al. 2016)	29.7	37.7	239	36.3	39.0	44.2	260	38.0	34.4	41.0	37.1
ConvNeXt-T(Liu et al. 2022)	135.2	-	-	-	-	-	262	-	-	46.2	41.7
PVT-Small(Wang et al. 2021c)	215.7	34.2	226	40.4	42.2	44.1	245	40.4	37.8	43.0	39.9
Swin-T(Liu et al. 2021)	-	38.5	245	41.5	43.9	47.8	264	42.2	39.1	46.0	41.6
Shuffle-T(Huang et al. 2021)	291.4	-	-	-	-	48.0	268	-	-	46.8	42.3
Twins-S(Chu et al. 2021a)	205.9	34.4	210	43.0	45.6	44.0	228	43.4	40.3	46.8	42.6
RegionViT-S(Chen et al. 2021b)	287.9	40.8	193	42.2	45.8	50.1	171	42.5	39.5	46.3	42.3
PVTv2-B2(Wang et al. 2021b)	387.7	35.1	231	44.6	-	45.0	-	45.3	41.2	-	-
PoolFormer-S36(Yu et al. 2022)	142.1	40.6	-	39.5	-	50.5	-	41.0	37.7	-	-
SepViT-T(ours)	241.8	45.4	243	44.8	46.8	54.7	261	45.5	41.9	48.0	43.8
ResNet101(He et al. 2016)	45.9	58.0	315	38.5	40.9	63.2	336	40.4	36.4	42.8	38.5
ResNeXt101-32×4d(Xie et al. 2017)	105.1	56.4	319	39.9	41.4	62.8	340	41.9	37.5	44.0	39.2
PVT-Medium(Wang et al. 2021c)	341.2	53.9	283	41.9	43.2	63.9	302	42.0	39.0	44.2	40.5
Swin-S(Liu et al. 2021)	-	59.8	335	44.5	46.3	69.1	354	44.8	40.9	48.5	43.3
Shuffle-S(Huang et al. 2021)	408.2	-	-	-	-	69.0	359	-	-	48.4	43.3
Twins-B(Chu et al. 2021a)	398.8	67.0	326	45.3	46.9	76.3	340	45.2	41.5	48.0	43.0
RegionViT-B(Chen et al. 2021b)	451.4	83.4	309	43.3	46.1	92.2	288	43.5	40.1	47.2	43.0
PVTv2-B3(Wang et al. 2021b)	439.1	55.0	288	45.9	-	64.9	-	47.0	42.5	-	-
SepViT-S(ours)	375.8	61.9	302	46.4	47.9	71.3	321	47.2	42.9	49.4	44.6

Table 4: Comparison of different backbones on object detection and instance segmentation tasks with RetinaNet and Mask R-CNN frameworks. Latency is the TensorRT runtime of the backbone with the input size of 800×800 (batch size=8). FLOPs are measured with the input size of 800×1280 . The superscript b and m denote the box detection and mask instance segmentation.

Model	DSSA	GSA	LWT	Param(M)	FLOPs(G)	Throughput(img/s)	Latency(ms)	Top-1 Acc(%)
Swin-T+CPVT (Chu et al. 2021a)				28.0	4.4	704	-	81.2
SepViT-T	✓			32.1	4.4	740	23.1	82.2
	✓	✓		31.2	4.5	729	24.5	82.5
	✓	✓	✓	31.2	4.5	729	24.5	82.7

Table 5: Ablation studies of the key components in our SepViT. LWT means the learnable window tokens.

Method	Param(M)	FLOPs(G)	Throughput(img/s)	Top-1 Acc(%)
Win_Tokens	31.2	4.5	729	82.7
Avg_Pooling	31.2	4.5	734	82.2
Dw_Conv	31.3	4.5	720	82.3

Table 6: Comparison of different approaches of getting the global representation of each window in SepViT.

fixed zero initialization scheme, the learnable window token (LWT) helps SepViT-T to boost the performance to 82.7%.

Window Token Embedding. To verify the effectiveness of learning the global representation of each window with our window token embedding scheme (Win_Tokens), we further study some other methods that directly get the global representations from the output feature maps of DSA, such as average pooling (Avg_Pooling) and depthwise convolution (DW_Conv). As the results illustrated in Table 6, our window token embedding scheme achieves the best performance among these approaches. Meanwhile, the comparison of parameters and FLOPs between Win_Token and Avg_Pooling methods demonstrates that our window token embedding scheme costs negligible computation.

Combination Types. We have studied the combinations of DSSA and GSA in SepViT. Particularly, we just apply GSA in the last few stages due to the high computation and

Block Type	Param(M)	FLOPs(G)	Throughput(img/s)	Top-1 Acc(%)
(D, D, D, D)	32.1	4.4	740	82.2
(D, D, D&G, D)	31.2	4.5	733	82.4
(D, D&G, D&G, D)	31.2	4.5	729	82.7
(D, G&D, G&D, D)	31.2	4.5	729	82.3

Table 7: Comparison of different combination types of DSSA (D) and GSA (G) in SepViT.

resolution in stage 1. As the result shows in Table 9, the best performance of 82.7% is achieved by putting DSSA before GSA and running them alternately in stage 2 and 3.

Conclusion

In this paper, we have presented an efficient Separable Vision Transformer, dubbed SepViT, which consists of three core designs. Firstly, depthwise separable self-attention enables SepViT to achieve information interaction within and among the windows in a single block. Next, window token embedding scheme helps SepViT to build the attention relationship among windows with negligible computational cost. Thirdly, the extended grouped self-attention enables SepViT to capture long-range visual dependencies across multiple windows for better performance. Experimental results on various vision tasks verify that SepViT achieves a state-of-the-art trade-off between performance and latency.

References

- Carion, N.; Massa, F.; Synnaeve, G.; Usunier, N.; Kirillov, A.; and Zagoruyko, S. 2020. End-to-end object detection with transformers. In *European Conference on Computer Vision*, 213–229.
- Chen, B.; Li, P.; Li, C.; Li, B.; Bai, L.; Lin, C.; Sun, M.; Yan, J.; and Ouyang, W. 2021a. Glit: Neural architecture search for global and local image transformer. In *Proceedings of the IEEE/CVF International Conference on Computer Vision*, 12–21.
- Chen, C.-F.; Panda, R.; Fan, Q.; and Chen. 2021b. Regionvit: Regional-to-local attention for vision transformers. *arXiv preprint arXiv:2106.02689*.
- Chen, M.; Peng, H.; Fu, J.; and Ling, H. 2021c. Autoformer: Searching transformers for visual recognition. In *Proceedings of the IEEE/CVF International Conference on Computer Vision*, 12270–12280.
- Chen, Y.; Dai, X.; Chen, D.; Liu, M.; Dong, X.; Yuan, L.; and Liu, Z. 2021d. Mobile-former: Bridging mobilenet and transformer. *arXiv preprint arXiv:2108.05895*.
- Chu, X.; Tian, Z.; Wang, Y.; Zhang, B.; Ren, H.; Wei, X.; Xia, H.; and Shen, C. 2021a. Twins: Revisiting the design of spatial attention in vision transformers. *arXiv preprint arXiv:2104.13840*.
- Chu, X.; Tian, Z.; Zhang, B.; Wang, X.; Wei, X.; Xia, H.; and Shen, C. 2021b. Conditional positional encodings for vision transformers. *arXiv preprint arXiv:2102.10882*.
- Dai, Z.; Cai, B.; Lin, Y.; and Chen, J. 2021. Up-detr: Unsupervised pre-training for object detection with transformers. In *Proceedings of the IEEE/CVF Conference on Computer Vision and Pattern Recognition*, 1601–1610.
- Dong, X.; Bao, J.; Chen, D.; Zhang, W.; Yu, N.; Yuan, L.; Chen, D.; and Guo, B. 2021. Cswin transformer: A general vision transformer backbone with cross-shaped windows. *arXiv preprint arXiv:2107.00652*.
- Dosovitskiy, A.; Beyer, L.; Kolesnikov, A.; Weissenborn, D.; Zhai, X.; Unterthiner, T.; Dehghani, M.; Minderer, M.; Heigold, G.; Gelly, S.; et al. 2020. An image is worth 16x16 words: Transformers for image recognition at scale. *arXiv preprint arXiv:2010.11929*.
- Graham, B.; El-Nouby, A.; Touvron, H.; Stock, P.; Joulin, A.; Jégou, H.; and Douze, M. 2021. LeViT: a Vision Transformer in ConvNet’s Clothing for Faster Inference. In *Proceedings of the IEEE/CVF International Conference on Computer Vision*, 12259–12269.
- Guo, J.; Han, K.; Wu, H.; Xu, C.; Tang, Y.; Xu, C.; and Wang, Y. 2021. Cmt: Convolutional neural networks meet vision transformers. *arXiv preprint arXiv:2107.06263*.
- Han, K.; Wang, Y.; Tian, Q.; Guo, J.; Xu, C.; and Xu, C. 2020. Ghostnet: More features from cheap operations. In *Proceedings of the IEEE/CVF Conference on Computer Vision and Pattern Recognition*, 1580–1589.
- Han, K.; Xiao, A.; Wu, E.; Guo, J.; Xu, C.; and Wang, Y. 2021. Transformer in transformer. *Advances in Neural Information Processing Systems*, 34.
- He, K.; Gkioxari, G.; Dollár, P.; and Girshick, R. 2017. Mask r-cnn. In *Proceedings of the IEEE International Conference on Computer Vision*, 2961–2969.
- He, K.; Zhang, X.; Ren, S.; and Sun, J. 2016. Deep residual learning for image recognition. In *Proceedings of the IEEE Conference on Computer Vision and Pattern Recognition*, 770–778.
- Howard, A.; Sandler, M.; Chu, G.; Chen, L.-C.; Chen, B.; Tan, M.; Wang, W.; Zhu, Y.; Pang, R.; Vasudevan, V.; et al. 2019. Searching for mobilenetv3. In *Proceedings of the IEEE/CVF International Conference on Computer Vision*, 1314–1324.
- Howard, A. G.; Zhu, M.; Chen, B.; Kalenichenko, D.; Wang, W.; Weyand, T.; Andreetto, M.; and Adam, H. 2017. Mobilenets: Efficient convolutional neural networks for mobile vision applications. *arXiv preprint arXiv:1704.04861*.
- Huang, G.; Sun, Y.; Liu, Z.; Sedra, D.; and Weinberger, K. Q. 2016. Deep networks with stochastic depth. In *European Conference on Computer Vision*, 646–661.
- Huang, Z.; Ben, Y.; Luo, G.; Cheng, P.; Yu, G.; and Fu, B. 2021. Shuffle transformer: Rethinking spatial shuffle for vision transformer. *arXiv preprint arXiv:2106.03650*.
- Kirillov, A.; Girshick, R.; He, K.; and Dollár, P. 2019. Panoptic feature pyramid networks. In *Proceedings of the IEEE/CVF Conference on Computer Vision and Pattern Recognition*, 6399–6408.
- Krizhevsky, A.; Sutskever, I.; and Hinton, G. E. 2012. Imagenet classification with deep convolutional neural networks. *Advances in Neural Information Processing Systems*, 25.
- Li, C.; Tang, T.; Wang, G.; Peng, J.; Wang, B.; Liang, X.; and Chang, X. 2021. Bossnas: Exploring hybrid cnn-transformers with block-wisely self-supervised neural architecture search. In *Proceedings of the IEEE/CVF International Conference on Computer Vision*, 12281–12291.
- Li, W.; Wen, S.; Shi, K.; Yang, Y.; and Huang, T. 2022. Neural architecture search with a lightweight transformer for text-to-image synthesis. *IEEE Transactions on Network Science and Engineering*, 1567–1576.
- Lin, T.-Y.; Goyal, P.; Girshick, R.; He, K.; and Dollár, P. 2017. Focal loss for dense object detection. In *Proceedings of the IEEE International Conference on Computer Vision*, 2980–2988.
- Lin, T.-Y.; Maire, M.; Belongie, S.; Hays, J.; Perona, P.; Ramanan, D.; Dollár, P.; and Zitnick, C. L. 2014. Microsoft coco: Common objects in context. In *European Conference on Computer Vision*, 740–755.
- Liu, Z.; Lin, Y.; Cao, Y.; Hu, H.; Wei, Y.; Zhang, Z.; Lin, S.; and Guo, B. 2021. Swin transformer: Hierarchical vision transformer using shifted windows. *arXiv preprint arXiv:2103.14030*.
- Liu, Z.; Mao, H.; Wu, C.-Y.; Feichtenhofer, C.; Darrell, T.; and Xie, S. 2022. A ConvNet for the 2020s. *arXiv preprint arXiv:2201.03545*.
- Loshchilov, I.; and Hutter, F. 2017. Decoupled weight decay regularization. *arXiv preprint arXiv:1711.05101*.

- Ma, N.; Zhang, X.; Zheng, H.-T.; and Sun, J. 2018. Shufflenet v2: Practical guidelines for efficient cnn architecture design. In *Proceedings of the European Conference on Computer Vision*, 116–131.
- Mehta, S.; and Rastegari, M. 2021. Mobilevit: light-weight, general-purpose, and mobile-friendly vision transformer. *arXiv preprint arXiv:2110.02178*.
- Russakovsky, O.; Deng, J.; Su, H.; Krause, J.; Satheesh, S.; Ma, S.; Huang, Z.; Karpathy, A.; Khosla, A.; Bernstein, M.; et al. 2015. Imagenet large scale visual recognition challenge. *International Journal of Computer Vision*, 115(3): 211–252.
- Sandler, M.; Howard, A.; Zhu, M.; Zhmoginov, A.; and Chen, L.-C. 2018. Mobilenetv2: Inverted residuals and linear bottlenecks. In *Proceedings of the IEEE Conference on Computer Vision and Pattern Recognition*, 4510–4520.
- Selvaraju, R. R.; Cogswell, M.; Das, A.; Vedantam, R.; Parikh, D.; and Batra, D. 2017. Grad-cam: Visual explanations from deep networks via gradient-based localization. In *Proceedings of the IEEE international conference on computer vision*, 618–626.
- So, D.; Le, Q.; and Liang, C. 2019. The evolved transformer. In *International Conference on Machine Learning*, 5877–5886.
- Tan, M.; and Le, Q. 2019. Efficientnet: Rethinking model scaling for convolutional neural networks. In *International Conference on Machine Learning*, 6105–6114.
- Touvron, H.; Cord, M.; Douze, M.; Massa, F.; Sablayrolles, A.; and Jégou, H. 2021. Training data-efficient image transformers & distillation through attention. In *International Conference on Machine Learning*, 10347–10357.
- Wang, H.; Zhu, Y.; Adam, H.; Yuille, A.; and Chen, L.-C. 2021a. Max-deeplab: End-to-end panoptic segmentation with mask transformers. In *Proceedings of the IEEE/CVF Conference on Computer Vision and Pattern Recognition*, 5463–5474.
- Wang, W.; Xie, E.; Li, X.; Fan, D.-P.; Song, K.; Liang, D.; Lu, T.; Luo, P.; and Shao, L. 2021b. Pvtv2: Improved baselines with pyramid vision transformer. *arXiv preprint arXiv:2106.13797*.
- Wang, W.; Xie, E.; Li, X.; Fan, D.-P.; Song, K.; Liang, D.; Lu, T.; Luo, P.; and Shao, L. 2021c. Pyramid vision transformer: A versatile backbone for dense prediction without convolutions. *arXiv preprint arXiv:2102.12122*.
- Wu, H.; Xiao, B.; Codella, N.; Liu, M.; Dai, X.; Yuan, L.; and Zhang, L. 2021. Cvt: Introducing convolutions to vision transformers. In *Proceedings of the IEEE/CVF International Conference on Computer Vision*, 22–31.
- Xiao, T.; Liu, Y.; Zhou, B.; Jiang, Y.; and Sun, J. 2018. Unified perceptual parsing for scene understanding. In *European Conference on Computer Vision*, 418–434.
- Xie, E.; Wang, W.; Yu, Z.; Anandkumar, A.; Alvarez, J. M.; and Luo, P. 2021. SegFormer: Simple and efficient design for semantic segmentation with transformers. *Advances in Neural Information Processing Systems*, 34.
- Xie, S.; Girshick, R.; Dollár, P.; Tu, Z.; and He, K. 2017. Aggregated residual transformations for deep neural networks. In *Proceedings of the IEEE Conference on Computer Vision and Pattern Recognition*, 1492–1500.
- Xu, W.; Xu, Y.; Chang, T.; and Tu, Z. 2021. Co-scale conv-attentional image transformers. In *Proceedings of the IEEE/CVF International Conference on Computer Vision*, 9981–9990.
- Yu, W.; Luo, M.; Zhou, P.; Si, C.; Zhou, Y.; Wang, X.; Feng, J.; and Yan, S. 2022. Metaformer is actually what you need for vision. In *Proceedings of the IEEE/CVF Conference on Computer Vision and Pattern Recognition*, 10819–10829.
- Yuan, L.; Chen, Y.; Wang, T.; Yu, W.; Shi, Y.; Jiang, Z.-H.; Tay, F. E.; Feng, J.; and Yan, S. 2021. Tokens-to-token vit: Training vision transformers from scratch on imagenet. In *Proceedings of the IEEE/CVF International Conference on Computer Vision*, 558–567.
- Zhang, X.; Zhou, X.; Lin, M.; and Sun, J. 2018. Shufflenet: An extremely efficient convolutional neural network for mobile devices. In *Proceedings of the IEEE Conference on Computer Vision and Pattern Recognition*, 6848–6856.
- Zheng, S.; Lu, J.; Zhao, H.; Zhu, X.; Luo, Z.; Wang, Y.; Fu, Y.; Feng, J.; Xiang, T.; Torr, P. H.; et al. 2021. Rethinking semantic segmentation from a sequence-to-sequence perspective with transformers. In *Proceedings of the IEEE/CVF Conference on Computer Vision and Pattern Recognition*, 6881–6890.
- Zhou, B.; Zhao, H.; Puig, X.; Fidler, S.; Barriuso, A.; and Torralba, A. 2017. Scene parsing through ade20k dataset. In *Proceedings of the IEEE Conference on Computer Vision and Pattern Recognition*, 633–641.
- Zhu, X.; Su, W.; Lu, L.; Li, B.; Wang, X.; and Dai, J. 2020. Deformable detr: Deformable transformers for end-to-end object detection. *arXiv preprint arXiv:2010.04159*.
- Zoph, B.; and Le, Q. V. 2016. Neural architecture search with reinforcement learning. *arXiv preprint arXiv:1611.01578*.

Appendix

Architecture Configurations

For fair comparison, we propose the SepViT-T/S/B variants. Moreover, we also design the SepViT-Lite variant with a very light model size. The specific configurations of SepViT variants are listed in Table 8, the block depth of SepViT is smaller in some stages than the competitors since SepViT is more efficient. DSSA and GSA denote the blocks with depthwise separable self-attention and grouped self-attention, respectively. Additionally, the expansion ratio of each MLP layer is set as 4, the window sizes are 7×7 and 14×14 for DSSA and GSA in all SepViT variants.

Configs	SepViT-Lite	SepViT-T	SepViT-S	SepViT-B
Blocks	[1, 2, 6, 2]	[1, 2, 6, 2]	[1, 2, 14, 2]	[1, 2, 14, 2]
Channels	[32, 64, 128, 256]	[96, 192, 384, 768]	[96, 192, 384, 768]	[128, 256, 512, 1024]
Heads	[1, 2, 4, 8]	[3, 6, 12, 24]	[3, 6, 12, 24]	[4, 8, 16, 32]
Block Type	[DSSA, DSSA&GSA, DSSA&GSA, DSSA]			

Table 8: Configurations of SepViT variants.

Comparison with Lite Models.

To further explore the potential of SepViT, we scale down SepViT to a lite model size (SepViT-Lite). As we can observe in Table 9, SepViT-Lite obtains an excellent top-1 accuracy of 72.3%, outperforming its counterparts with similar model sizes.

Method	Param(M)	FLOPs(G)	Top-1 Acc(%)
MobileNet-V2 (Sandler et al. 2018)	3.4	0.3	71.8
ResNet18 (He et al. 2016)	11.1	1.8	69.8
PVTv2-B0 (Wang et al. 2021b)	3.4	0.6	70.5
SepViT-Lite	3.7	0.6	72.3

Table 9: Comparison of lite models on classification.

Implementation Details

ImageNet-1K Classification. Image classification experiment is conducted on ImageNet-1K (Russakovsky et al. 2015), which contains about 1.28M training images and 50K validation images from 1K categories. For a fair comparison, we follow the training settings of the recent vision Transformer (Chu et al. 2021a). Concretely, all of the SepViT variants are trained for 300 epochs on 8 V100 GPUs with a total batch size of 1024. The resolution of the input image is resized to 224×224 . We adopt the AdamW (Loshchilov and Hutter 2017) as the optimizer with weight decay 0.1 for SepViT-B and 0.05 for SepViT-S/T. The learning rate is gradually decayed based on the cosine strategy with the initialization of 0.001. We use a linear warm-up strategy with 20 epochs for SepViT-B and 5 epochs for SepViT-S/T. Besides, we have also employed the increasing stochastic depth augmentation (Huang et al. 2016) with the maximum drop-path rate of 0.2, 0.3, 0.5 for our SepViT-T/S/B models.

Semantic Segmentation. Segmentation experiment is carried out on ADE20K (Zhou et al. 2017), which contains about 20K training images and 2K validation images from 150 categories. To make fair comparisons, we also follow the training conventions of the previous vision Transformers (Chu et al. 2021a) on the Semantic FPN (Kirillov et al. 2019) and UperNet (Xiao et al. 2018) frameworks. All of our models are pre-trained on the ImageNet-1k and then finetuned on ADE20K with the input size of 512×512 . For the Semantic FPN framework, we adopt the AdamW optimizer with both the learning rate and weight decay being 0.0001. Then we train the whole networks for 80K iterations with the total batch size of 16 based on the stochastic depth of 0.2, 0.3, and 0.4 for SepViT-T/S/B. For the training and testing on the UperNet framework, we train the models for 160K iterations with the stochastic depth of 0.3, 0.3, and 0.5. AdamW optimizer is used as well but with the learning rate 6×10^{-5} , total batch size 16 and weight decay 0.01 for SepViT-T/S and 0.03 for SepViT-B. Then we test the mIoU based on both single-scale and multi-scale (MS) where the scale goes from 0.5 to 1.75 with an interval of 0.25.

Object Detection and Instance Segmentation. Object detection and instance segmentation is implemented (Lin et al. 2014) based on the RetinaNet (Lin et al. 2017) and Mask R-CNN (He et al. 2017) frameworks with COCO (Lin et al. 2014). Specifically, all of our models are pre-trained on ImageNet-1K and then finetuned following the settings of the previous works (Chu et al. 2021a). As for the $1\times$ experiment, both the RetinaNet-based and the Mask R-CNN-based models use the AdamW optimizer with the weight decay 0.001 for SepViT-T and 0.0001 for SepViT-S. And they are trained with the total batch size of 16 based on the stochastic depth of 0.2 and 0.3 for SepViT-T/S. During the training, there are 500 iterations for warm-up and the learning rate will decline by $10\times$ at epochs 8 and 11. For the $3\times$ experiment with multi-scale (MS) training, models are trained with the resized images such that the shorter side ranges from 480 to 800 and the longer side is at most 1333. Moreover, most of all the other settings are the same as the $1\times$ except that the stochastic depth is 0.3 for SepViT-T, the weight decay becomes 0.05 and 0.1 for SepViT-T/S, and the decay epochs are 27 and 33.